

Kenjiro KOMAI*, Kohji MINOSHIMA* and Shigeyoshi SATOH**

Fatigue Fracture Behavior of SiC Whisker / Aluminum Matrix Composite under In-Phase and Out-of-Phase Tension/Torsion Loading

* Depart. Mech. Eng., Kyoto University, Kyoto 606-01, JAPAN.

** West Japan Railway Company, Osaka, JAPAN.

Keywords: Metal Matrix Composite, Fatigue, Crack Initiation, Whisker

ABSTRACT: This paper describes an investigation on the fatigue fracture behavior of an SiC whisker reinforced A6061 aluminum alloy fabricated by a squeeze casting process under in-phase and out-of-phase combined tension/torsion loading at room temperature. The tests were conducted under a load-controlled condition keeping a constant value of the combined stress ratio, $\alpha = \tau_{max} / \sigma_{max}$. Irrespective of loading condition, mechanical properties of the composite including fatigue strength were superior to those of an unreinforced A6061 alloy, not only under uniaxial loading, but also under combined in-phase and out-of-phase tension/torsion loading. As for unreinforced matrix material, fatigue strength under out-of-phase combined loading was smaller than that under in-phase loading. However, for the composite, fatigue strength under out-of-phase combined loading was higher than that under in-phase loading. Crack initiation and propagation behavior was closely examined by using a surface replication technique, and fracture mechanisms under in-phase and out-of-phase combined loading were discussed.

Introduction

Continuous progress in science and technology creates increasing demand for further improved structural materials; the mechanical properties required in many technological fields are high-strength, low-specific density, high wear resistance, and also heat-resistant property. Of various structural materials, metal matrix composites have attracted engineers and researchers because of their potentials to meet such demands. Especially short fiber such as whisker reinforced metals are easy for machining compared to continuous fiber reinforced metals. Many researches have been performed on strengthening mechanisms (1), fracture and fatigue (2-6) behavior, and also environmental influences on fracture (4) and corrosion behavior (7). However, fracture behavior under combined loading are scarcely reported (5),

although it is important from the standpoints of the application of a composite to machines and structures.

In this investigation, the authors have conducted quasi-static and fatigue tests of an SiC whisker reinforced aluminum alloy under combined tension/torsion loading at room temperature. Special attention was paid to the effects of in-phase and out-of-phase tension/torsion loading on fatigue fracture behavior. Crack initiation and propagation were closely examined by using a replication technique, and the fracture mechanisms of the composite are discussed.

Experimental procedures

The material tested was an SiC whisker reinforced A6061 aluminum alloy ($V_f = 17\%$). The composite, which was heat-treated to a T6 condition, was fabricated through a squeeze casting process, with final extrusion rate of 28, and thus most whisker aligned in the longitudinal direction. The average diameter of the whisker was $0.84\mu\text{m}$, and the average length after processing was $4.86\mu\text{m}$.

Smooth specimens shown in Fig. 1 were machined in the longitudinal direction, i.e., extruding direction. The specimens were polished with emery papers (#1500) followed with final finish with a diamond paste. The testing machine employed was a computer-controlled electro-hydraulic tension-torsion fatigue testing machine (load capacity: $\pm 100\text{kN}$, $\pm 1\text{kN}\cdot\text{m}$).

Static and fatigue tests under combined tension/torsion loading were conducted at room temperature for both composite and unreinforced matrix material. Static tests were conducted under a load-controlled condition keeping a constant value of a combined stress ratio, $\alpha = \tau/\sigma$, where σ is the axial stress and τ the torsional stress. Fatigue tests at a stress ratio of 0.1 were performed at a frequency of 5 Hz under in-phase (phase angle between tension and torsion

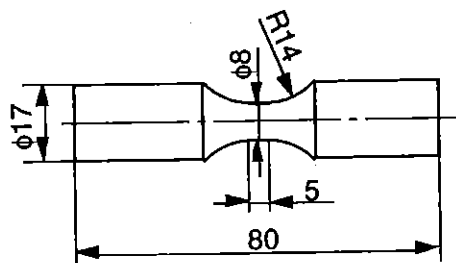


Fig.1 Shape and dimensions of test specimens. All dimensions are in mm.

loading, ϕ , of 0°) and out-of-phase ($\phi = 180^\circ$) combined tension/torsion loading. The tests were conducted under a load-controlled condition keeping a constant value of a combined stress ratio, $\alpha = \tau_{\max} / \sigma_{\max}$, where σ_{\max} is the maximum axial stress and τ_{\max} the maximum torsional stress in a cycle. Crack initiation and growth behavior were closely examined by using surface replication technique. Fracture surfaces were closely examined with scanning electron microscopes (HFS-2 by Hitachi, and JSM-5400LV by JEOL).

Experimental results and discussions

Quasi-static fracture behavior

Figure 2 shows the static strengths under in-phase combined loading, which are plotted in relation of axial stress and torsional stress. The arrows in the figure indicate that specimens did not completely fracture even though the maximum torsional angle (about ± 50 degrees) was applied to the specimen. The solid lines shown in the figure are the predicted failure strengths by Tsai-Hill failure criterion (8), derived by tensile ($\alpha=0$) and torsional ($\alpha=\infty$) strengths: the static strength of both composite and unreinforced matrix material showed good agreement with the Tsai-Hill failure criterion. The second point we must note is that the static strength of the composite was superior to that of an unreinforced A6061 alloy, not only

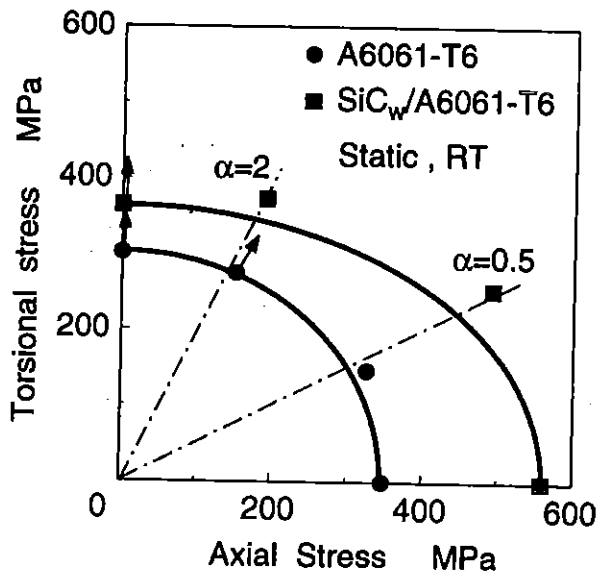


Fig.2 Quasi-static strength under tension/torsion combined loading.

under uniaxial loading, but also under combined tension/torsion loading (5).

Fatigue fracture behavior

Figures 3 (a) and (b) respectively show S-N curves under uniaxial and torsional loading. The fatigue strength of the composite under both loading conditions was higher than those of unreinforced matrix material, and it is clear that whisker reinforcements are very effective to increase fatigue strength of the composite.

Figure 4 shows S-N curves under in-phase and out-of-phase combined tension/torsion loading, plotted against maximum axial stress. As for matrix material, the fatigue strength under out-of-phase combined loading was lower than that under in-phase combined loading, irrespective of α value. This result is consistent with those reported for unreinforced metals (9, 10). However, for the composite, the fatigue strength under out-of-phase loading was superior to those under in-phase loading.

Macroscopic fracture morphology under tension/torsion combined loading

Under combined tension/torsion loading, the maximum stress is always in the specimen surface, and hence the crack initiation site was in the specimen surface. For both: matrix material and composite under combined tension/torsion loading, a crack that led final failure was in a plane where the maximum shear stress existed. We must note that there are two plane where the shear stress takes the maximum: of these two planes, the final failure was resulted from a crack in a plane which was near the longitudinal, or axial direction, except for matrix material under out-of-phase loading. In the case of matrix material under out-of-phase loading, the final failure was brought about by a crack in maximum shear plane near the transverse direction.

Crack initiation and propagation behavior

As is discussed before, an influence of out-of-phase tension/torsion loading on fatigue strength and macroscopic fracture morphology differed between in the matrix material and

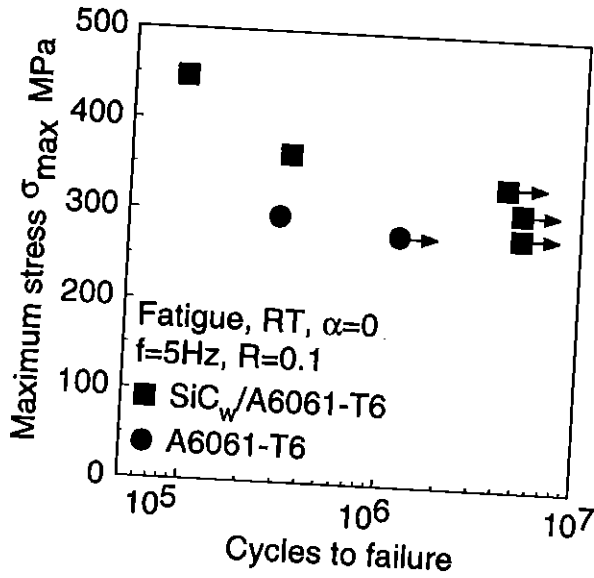


Fig.3(a) S-N curves under uniaxial loading.

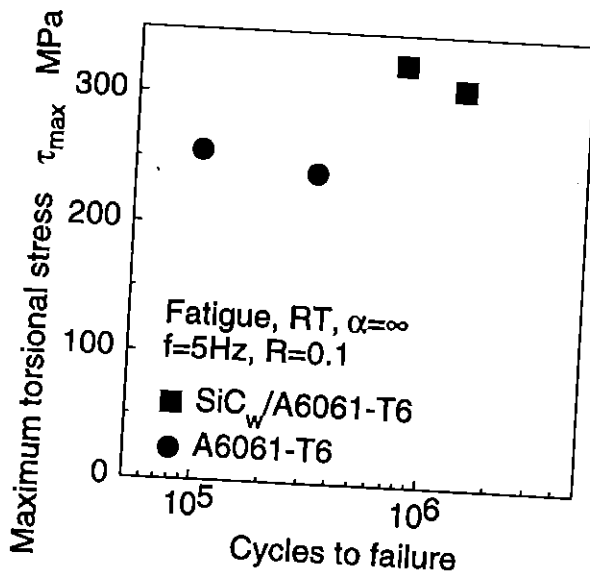
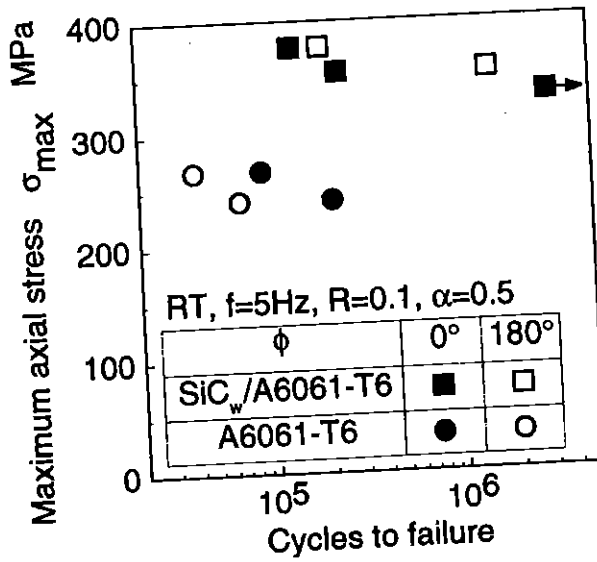
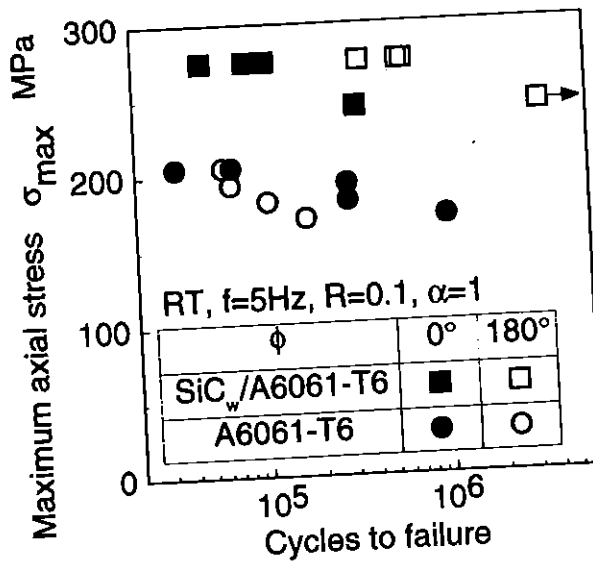


Fig.3(b) S-N curves under torsional loading.

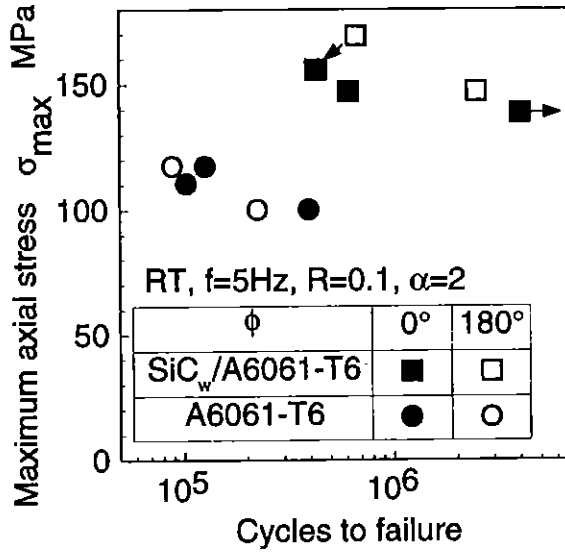


(a) $\alpha = 0.5$



(b) $\alpha = 1$

Fig.4 S-N curves under tenslon/torsion combined loading.



(c) $\alpha = 2$

Fig.4 S-N curves under tension/torsion combined loading.

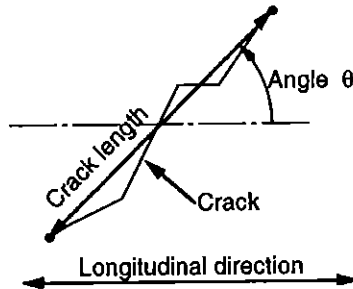
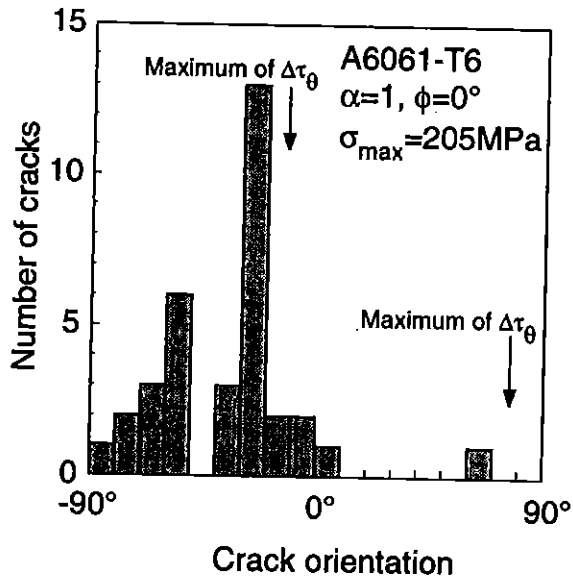


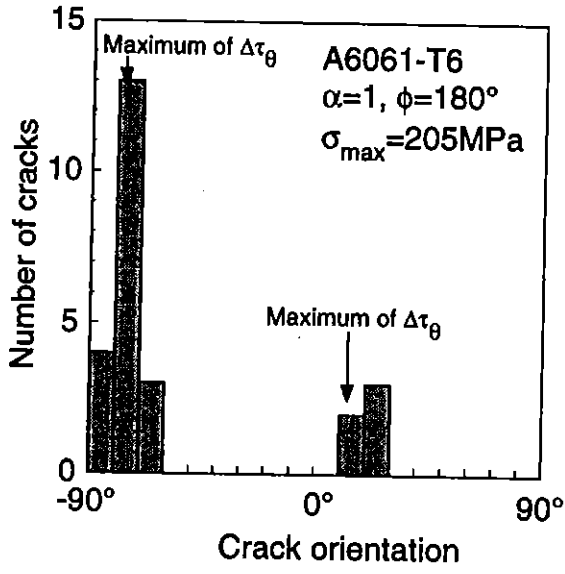
Fig.5 Definition of crack length and crack orientation.

the composite. Therefore, crack initiation and propagation behavior was closely examined by replication technique, selecting the loading condition of $\alpha = 1$. In this investigation, crack length and crack orientation was defined as is shown in Fig. 5.

Crack initiation orientation. The results of crack initiation orientation are summarized in Fig. 6 (matrix material) and Fig. 7 (composite). For both materials, most of the cracks were initiated in a plane where shear stress took the maximum. For the matrix material, most

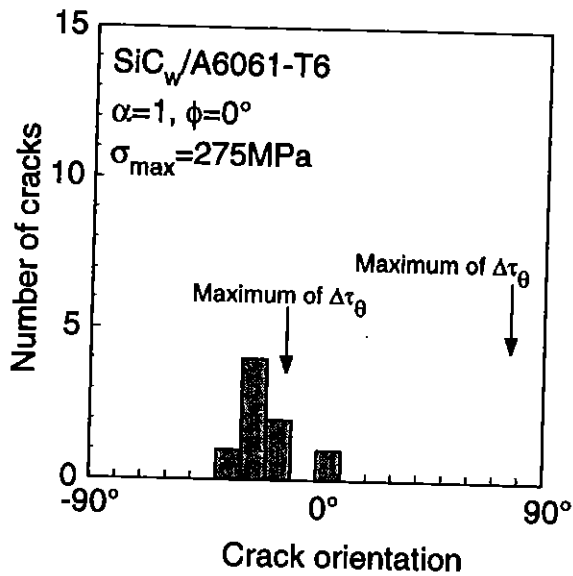


(a) In-phase combined loading

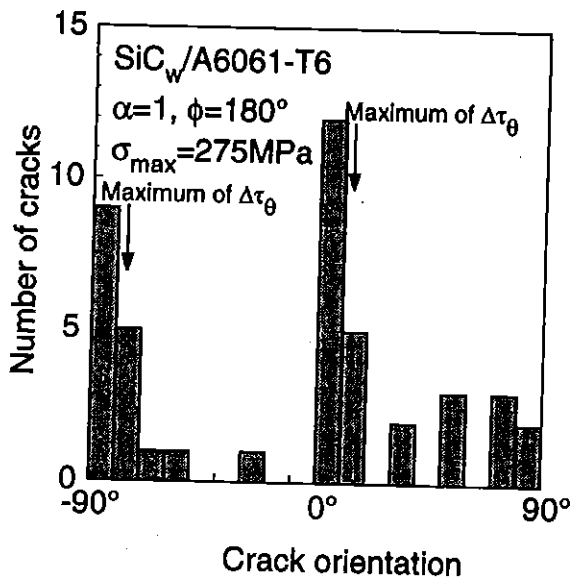


(b) out-of-phase combined loading

Fig.6 Crack initiation orientation of A6061 Al alloy. ($\alpha = 1$)



(a) in-phase combined loading



(b) out-of-phase combined loading

Fig.7 Crack initiation orientation of SiC_w/A6061. ($\alpha=1$)

of cracks under in-phase tension/torsion loading were in a plane which was near longitudinal direction (L-type crack), whereas under out-of-phase loading, most of cracks were in a plane near transverse direction (T-type crack). As for the composite, most of cracks were L-type cracks under in-phase tension/torsion loading. Under out-of-phase loading, both L and T-type cracks were observed. Unlike the matrix material, however, L-type cracks were more dominant than T-type crack.

Crack growth behavior. Figures 8 and 9 respectively show changes in crack length of the matrix material and the composite with stress cycles. In Fig.8, changes in L-type crack are shown for in-phase loading, whereas those in T-type crack are shown for out-of-phase loading, both of which respectively caused final failure. Figure 9(a) summarizes the changes in L-type crack which led final failure of the composite under both in-phase and out-of-phase loading, whereas Fig.9(b) shows changes in L and T-type cracks, which were observed under out-of-phase tension/torsion loading. For the matrix material, T-type cracks observed under out-of-phase loading were initiated earlier, and propagated faster than L-type cracks observed under in-phase loading. This fairly well agreed with the results that fatigue strength under out-of-phase loading was lower than that under in-phase loading.

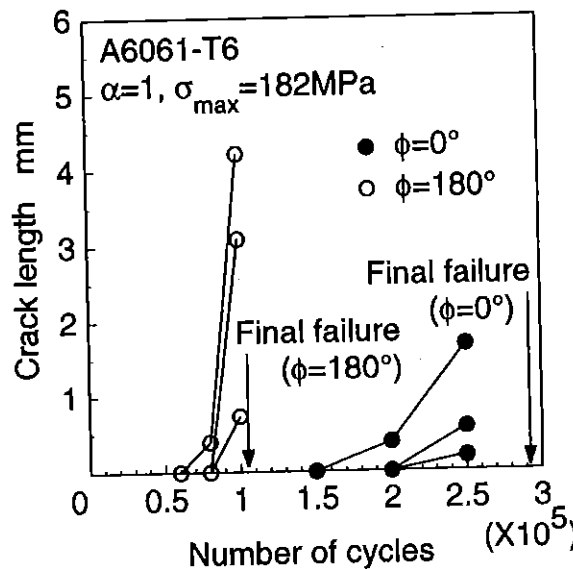
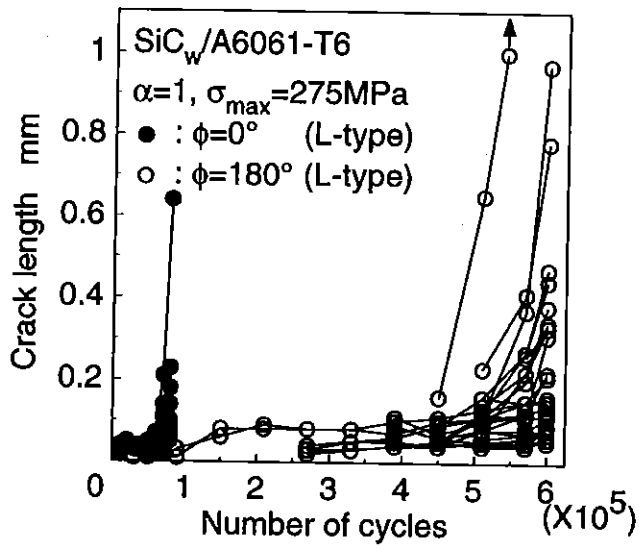
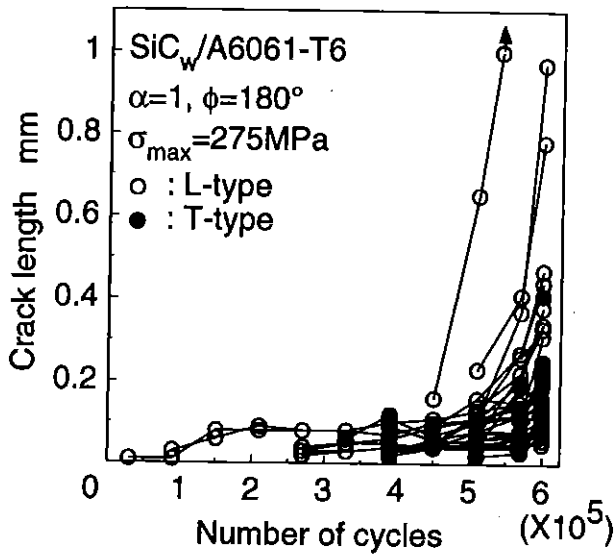


Fig.8 Crack growth curves in A6061 Al alloy under in-phase and out-of-phase combined loading. (In-phase loading: L-type crack, Out-of-phase loading: T-type crack.)



(a) Changes in L-type crack under in-phase and out-of-phase loading.



(b) Comparison between L- and T-type crack growth behavior under out-of-phase loading.

Fig.9 Crack growth curves in $\text{SiC}_w/\text{A6061}$ under combined loading.

As for the composite, crack growth rate of L-type crack, which led final failure, was faster under in-phase loading than under out-of-phase loading (see Fig.9(a)). Under out-of-phase loading, L-type crack growth rate was higher than that of T-type crack, indicating that L-type crack was easy to propagate than T-type crack. When we compare the crack growth behavior between the matrix material and the composite, a noticeable difference is that crack initiated earlier at about 10% of fatigue lives in the composite than in the matrix material, and most of fatigue lives of the composite were dominated by fatigue growth stage.

Fracture surface morphology

In the case of the matrix material, striations could be observed under both in-phase and out-of-phase loading. However, a difference of fracture morphology between under uniaxial loading and tension/torsion loading was that fracture surface rubbed each other, in particular under out-of-phase loading, and tire truck and rub marks were observed.

As for composite material, a T-type crack was initiated at a whisker end, and propagated with zig-zag path avoiding whisker. An L-type crack was initiated at whisker/matrix interface, and some whiskers could be observed in a fracture surface. However, similarly to the matrix material, fracture surfaces rubbed each other, and surface contact-induced debris were observed in L-type crack fracture surface. In the case of T-type cracks, some tire trucks and rub marks were observed.

Influence of out-of-phase loading on fatigue strength

In the case of matrix material under out-of-phase loading, cracks were initiated earlier and propagated faster, resulting in lower fatigue strength than under in-phase loading. T-type cracks under out-of-phase loading were initiated in the plane where a positive stress range was larger in two planes where shear stress took the maximum. Out-of-phase tension/torsion loading induced rotation of maximum principal stress, which caused interaction of slip planes, resulting in severe fatigue damage. This type of severe fatigue damage was already reported in unreinforced metals (10, 11). This is a reason why the fatigue strength of unreinforced matrix material under out-of-phase tension/torsion loading became smaller than under in-phase loading.

As for the composite under both in-phase and out-of-phase tension/torsion loading, L-type

cracks were initiated by whisker/matrix interfacial debonding at early stage of about 10% of fatigue lives, and most of fatigue lives were dominated by fatigue crack growth stage. At the same time, L-type crack growth rate under out-of-phase loading became smaller than under in-phase loading. This is a reason why the fatigue strength under out-of-phase loading was higher than that under in-phase loading.

In the case of matrix material under out-of-phase loading, T-type cracks were initiated and propagated. However, for the composite material, L-type cracks were initiated more than T-type cracks, because of anisotropy of the composite material; when an SiC_w/Al was subjected to uniaxial loading, crack growth rate in the T-L or R-L crack plane orientation was higher than that in L-T or L-R crack plane orientation (2, 3). Therefore, L-type cracks were initiated more than T-type cracks, and propagated faster, although the positive normal stress range was smaller in a plane of L-type crack. Comparing crack growth rate of L-type crack between under in-phase and out-of phase loading, positive stress range of normal stress under out-of-phase loading was smaller than that under in-phase loading, resulting in lower crack growth rate under out-of-phase loading than under in-phase loading. This is a reason, why fatigue strength under out-of-phase loading was higher than that under in-phase loading.

Conclusions

Fatigue tests of an SiC whisker reinforced A6061 aluminum alloy and its matrix material (A6061 aluminum alloy) under in-phase ($\phi = 0^\circ$) and out-of-phase ($\phi = 180^\circ$) combined tension/torsion loading at room temperature were performed. The tests were conducted with various combined stress ratios $\alpha (= \tau_{\max}/\sigma_{\max})$, and crack initiation and propagation behavior was closely examined by using replication technique. The investigation yielded the following conclusions:

1. The quasi-static strength and fatigue strength of the composite under combined tension/torsion loading were superior to those of unreinforced matrix material.
2. Fatigue strength of matrix material under in-phase loading was higher than that under out-of-phase combined loading. However, the fatigue strength of the composite under in-phase combined loading was smaller than that under out-of-phase combined loading.

3. Under in-phase and out-of-phase combined loading, a crack that led final failure was in a plane near the longitudinal direction, where shear stress took the maximum (L-type crack), except for the matrix material under out-of-phase loading. In this case, final failure was brought about by a crack in maximum shear plane near the transverse direction, i.e., T-type crack.
4. As for matrix material, T-type cracks under out-of-phase combined loading were initiated earlier and propagated faster than L-type cracks under in-phase combined loading, resulting in lower fatigue strength under out-of-phase loading.
5. L-type crack led final failure of the composite material, irrespective of loading mode, because of anisotropy of the material. Positive normal stress range of L-type crack under out-of-phase loading was smaller than that under in-phase loading, resulting in lower crack growth rate, i.e., higher fatigue strength.

References

- (1) Arsenault, R.J., (1988), The strengthening mechanisms in discontinuous SiC/Al composites. *Mechanical and Physical Behavior of Metallic and Ceramic Composite*, pp. 279-284. Risø National Laboratory.
- (2) Shang, J.K. and R.O. Ritchie, (1991), Fatigue of discontinuously reinforced metal matrix composites. *Metal Matrix Composites: Mechanisms and Properties*, (Edited by Everett, R.K. and Arsenault R.J.), pp.255-285, Academic Press.
- (3) Hirano, K. and Takizawa, S., (1989), Evaluation of fatigue crack growth characteristics of whisker reinforced metals, *Trans. Japan Soc. Mech. Eng., Series A.*, vol.55, pp.373-379.
- (4) Komai, K., Minoshima, K., and H. Ryoson, (1993), Tensile and Fatigue Fracture Behavior and Water-Environment Effects in SiC-Whisker/7075-Aluminum Composite, *Composi. Sci. Tech.*, vol.46, pp.59-66.
- (5) Komai, K., Minoshima, K., and G. Yoshida, (1994), Fracture behavior of SiC whisker reinforced aluminum alloy under combined tension/torsion loading at room and elevated temperatures, *Trans. Japan Soc. Mech. Eng., Series A.*, vol.60, pp.1080-1087.
- (6) Ishii, H., Yano, A., and Tohgo, K., (1996), Torsional fatigue of whisker or SiC particle reinforced 6061 aluminum alloy, *Jour. Soc. Mater. Sci., Japan*, vol.45, pp.60-63.
- (7) Hihara, L.H. and R.M. Latanision, (1992), Galvanic corrosion of aluminum-matrix composites, *Corrosion*, vol.48, pp.546-552.
- (8) Tsai, S.W., (1966), Air Force Materials Laboratory Report, AMFR-TR-66-149.
- (9) Kanazawa, K., Miller, K.J., and Brown, M.B., (1977), Low-cycle fatigue under out-of-phase loading conditions, *Jour. Eng. Mater. Tech*, vol.99, pp.222-228.
- (10) Chen, X., Gao, Q., and Sun, X.F., (1994), Damage analysis of low-cycle fatigue under non-proportional loading, *Fatigue*, vol.16, pp.221-225.
- (11) Socie, D., (1987), Multiaxial fatigue damage models, *Jour. Eng. Mater. Tech.*, vol.109, pp.293-305.